Supporting Information for

Phase-Tailored CoCrFeNiAl-Nitride for Enhanced Electrocatalytic Hydrogen Evolution Behavior via Cooling-Mediated Plasma Strategy

Bo Ouyang[a,#], Haonan Qin[a,#], Fengkun Li[b], Chen Li[c], Zhaofu Du[d], Yongqi Zhang[c], Li Yang[e], Erjun Kan[a,*], Kun Xu[f], Zhishan Mi[e,**],

[a] MIIT Key Laboratory of Semiconductor Microstructure and Quantum Sensing, School of Science, Nanjing University of Science and Technology, Nanjing 210094, China
[b] School of Energy and Mechanical Engineering, Dezhou University, Dezhou, 253023, China
[c] Institute of Fundamental and Frontier Sciences, University of Electronic Science and Technology of China, Chengdu 611371, China
[d] Beijing Aerospace Micro-Electronics Technology Co.Ltd, Beijing Institute of Radio Measurement, Beijing 1000039, China
[e] Research Institute of Advanced Materials (Shenzhen) Co., Ltd., Shenzhen 518045, China
[f] School of Chemistry and Chemical Engineering, Key Laboratory of Functional Inorganic Material Chemistry of Anhui Province, Anhui University, Hefei, Anhui 230601, China

# These authors contribute equally to this work.
* corresponding authors:
ekan@njust.edu.cn (Erjun Kan)
mizhishan@163.com (Zhishan Mi)

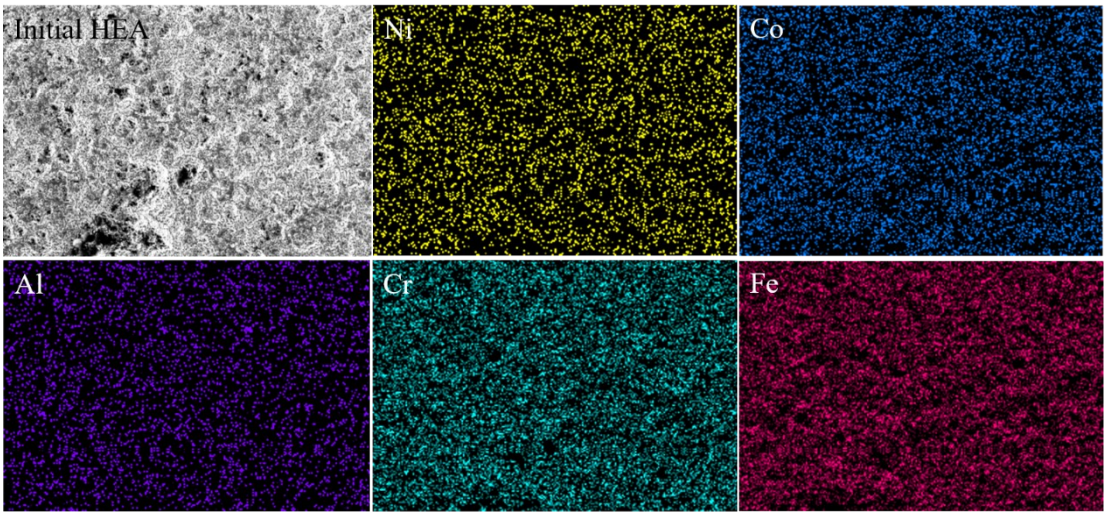

Figure S1. SEM-EDX mapping of initial HEA.

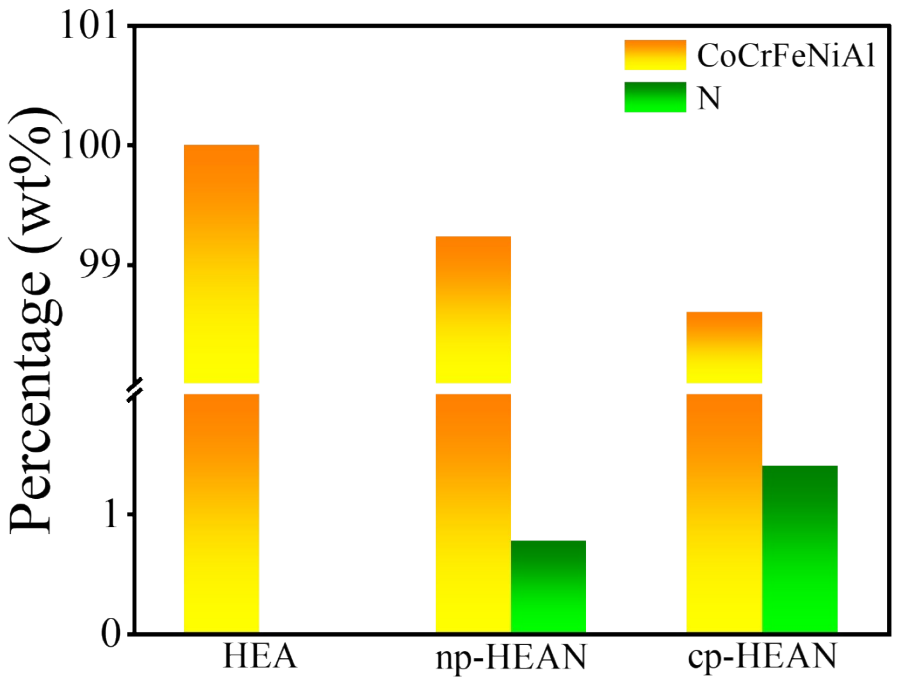

Figure S2. Species percentage comparison of HEA, np-HEAN and cp-HEAN based on SEM-EDX mapping.

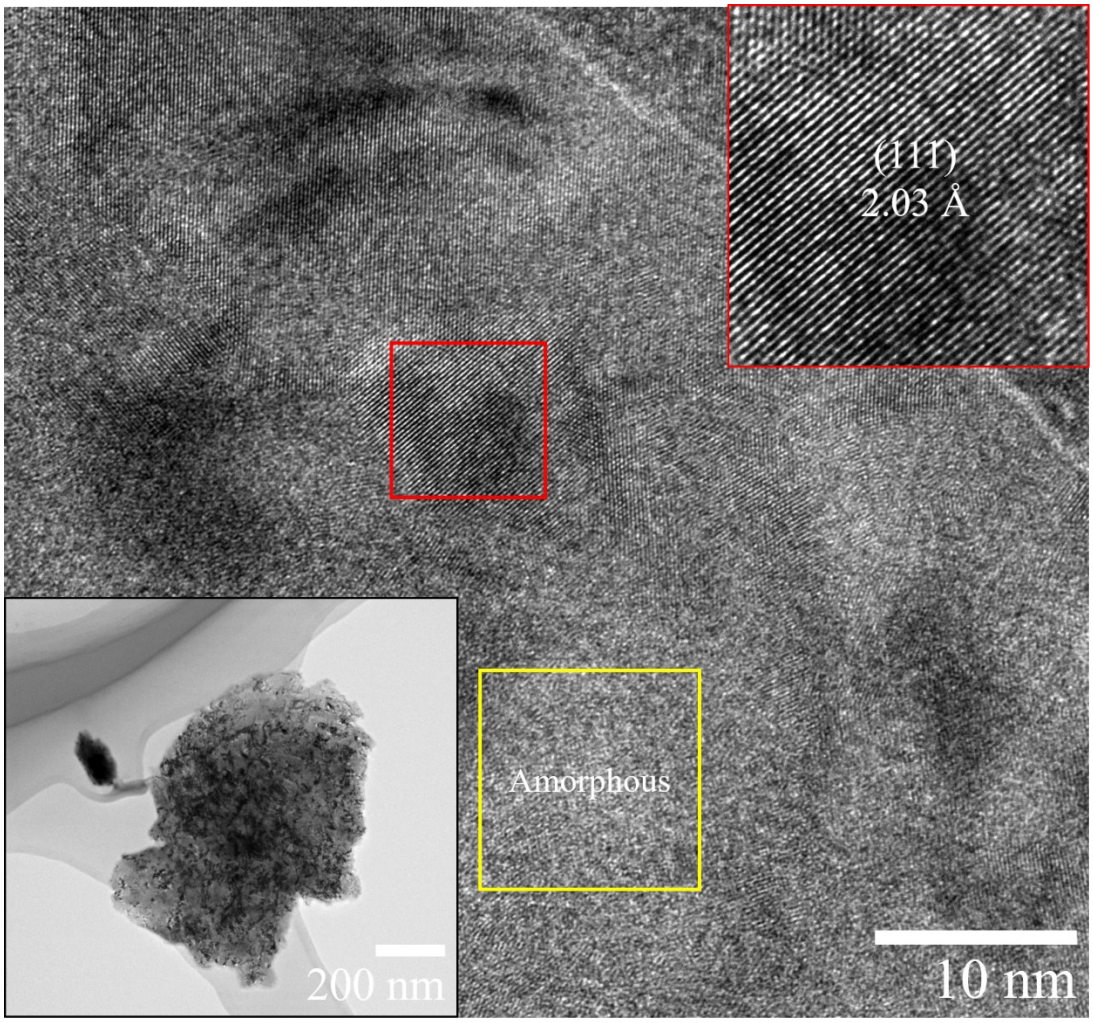

Figure S3. TEM images of initial HEA.

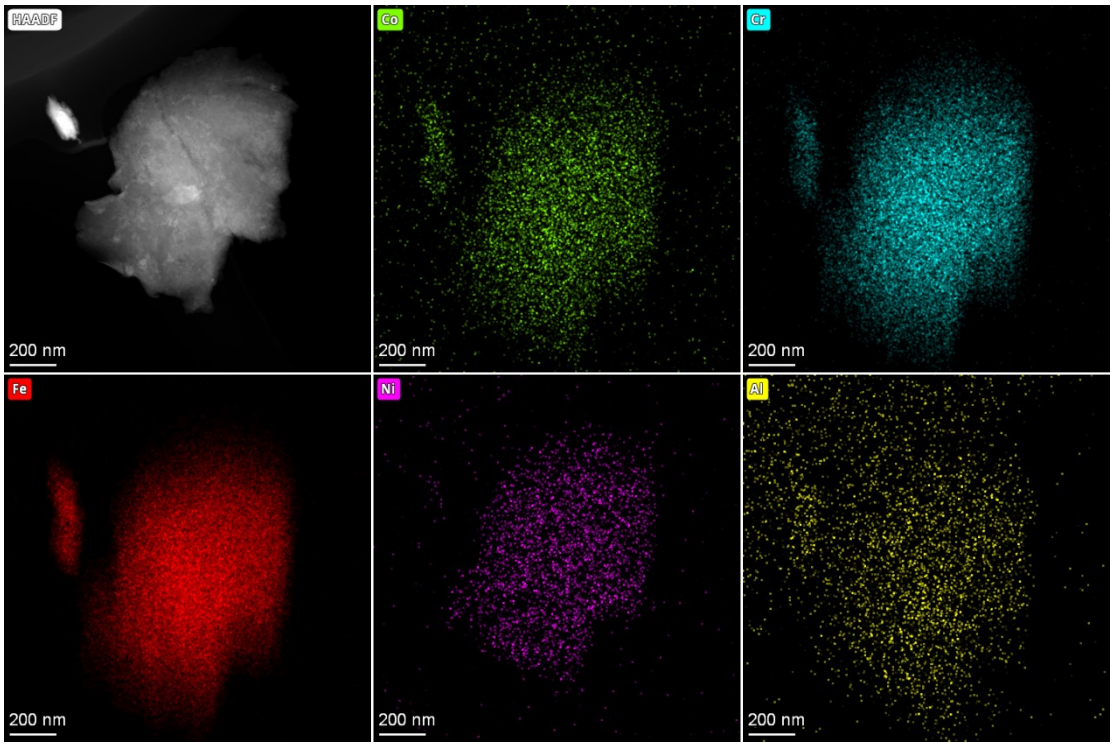

Figure S4. TEM-EDX mapping of initial HEA.

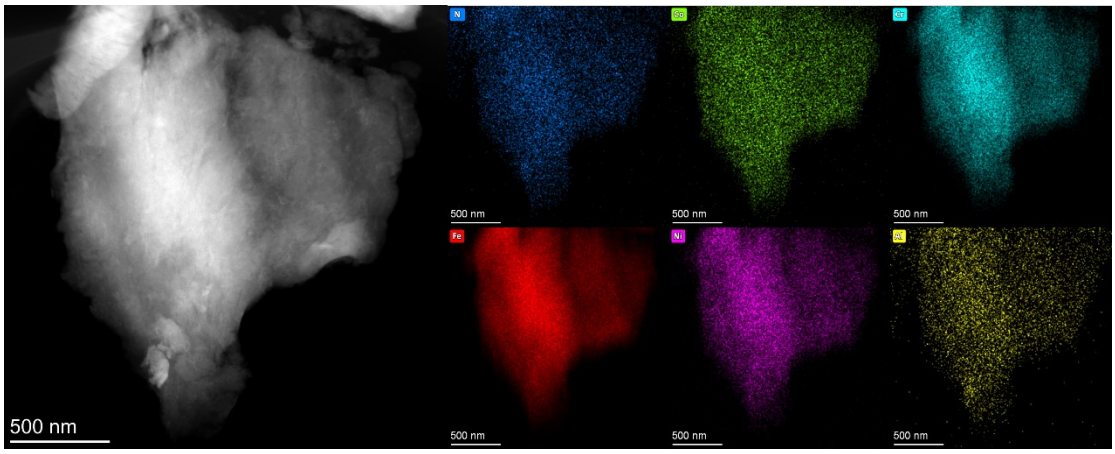

Figure S5. TEM-EDX mapping of np-HEAN.

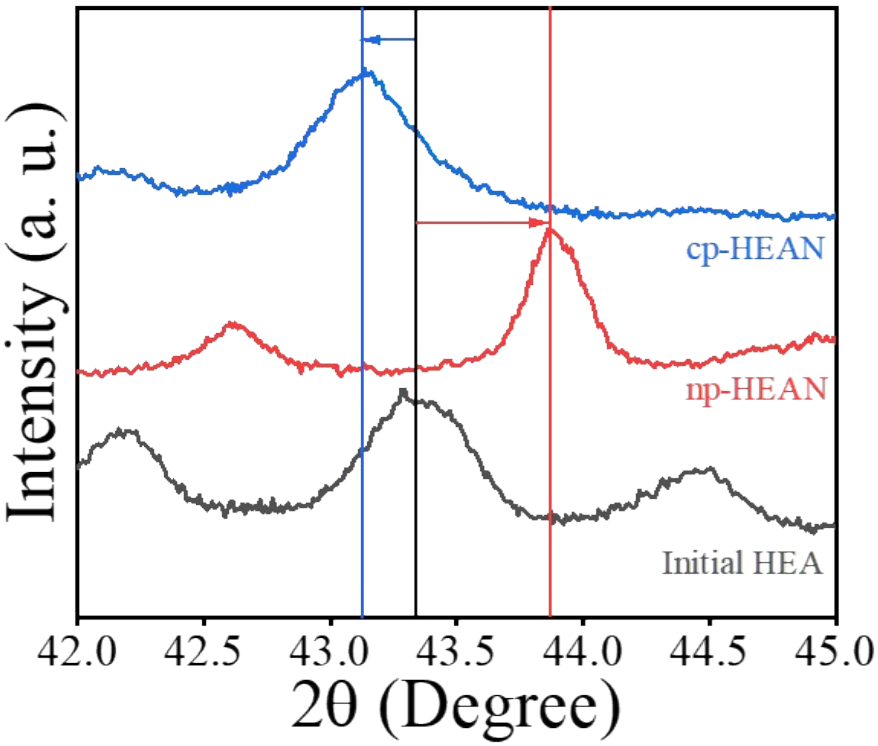

Figure S6. Magnified XRD patterns OF HEA, np-HEAN and cp-HEAN.

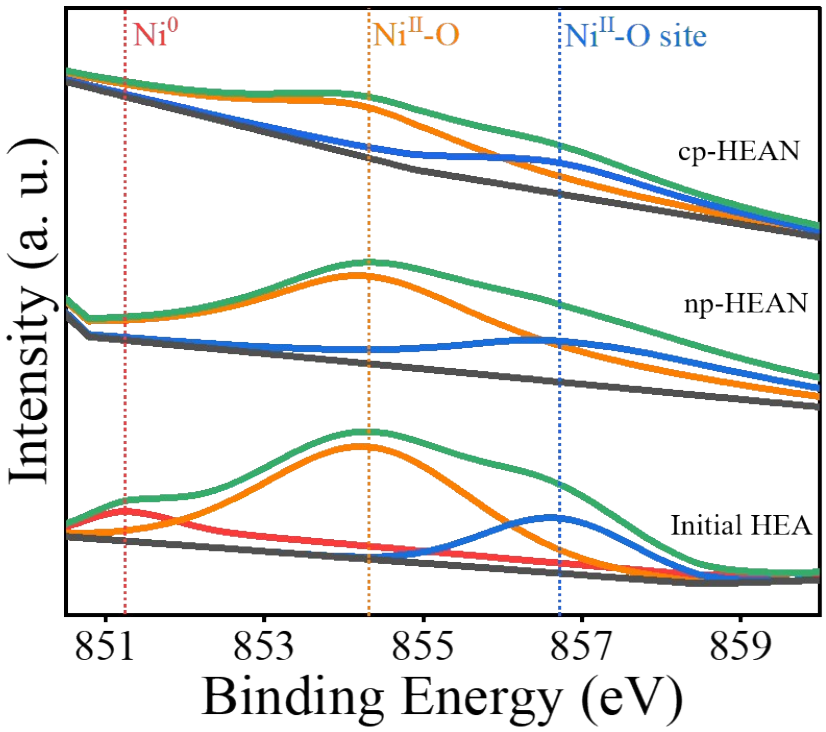

Figure S7. XPS Ni 2p spectra OF HEA, np-HEAN and cp-HEAN.

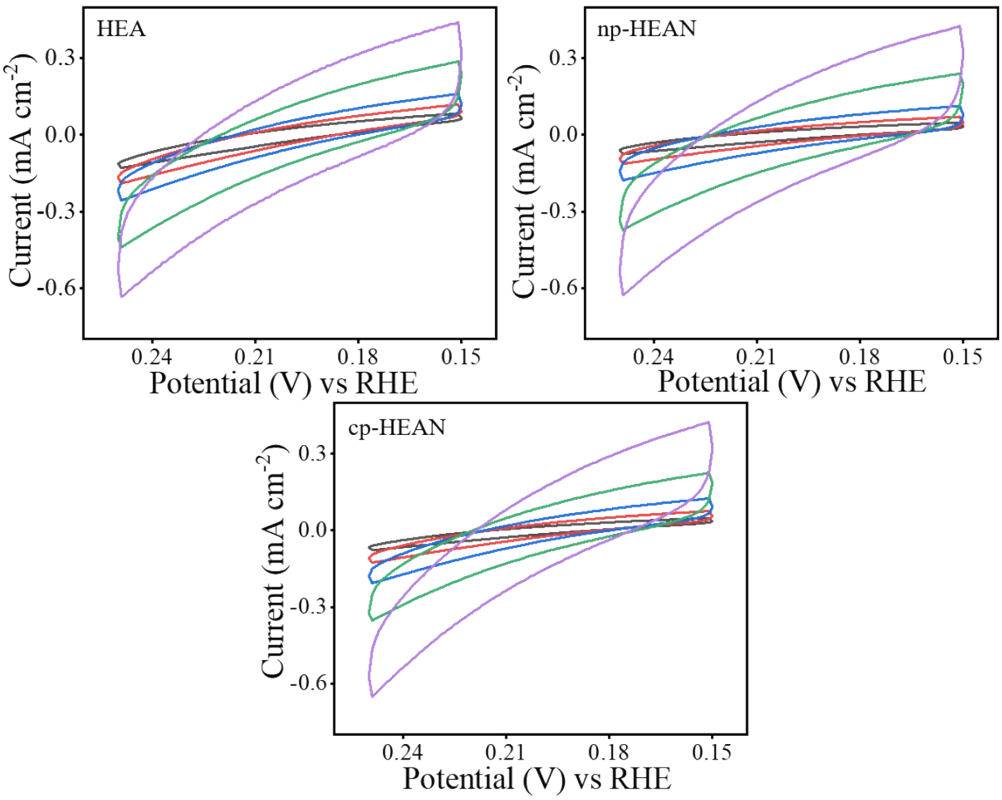

Figure S8. CV curves of HEA, np-HEAN and cp-HEAN.

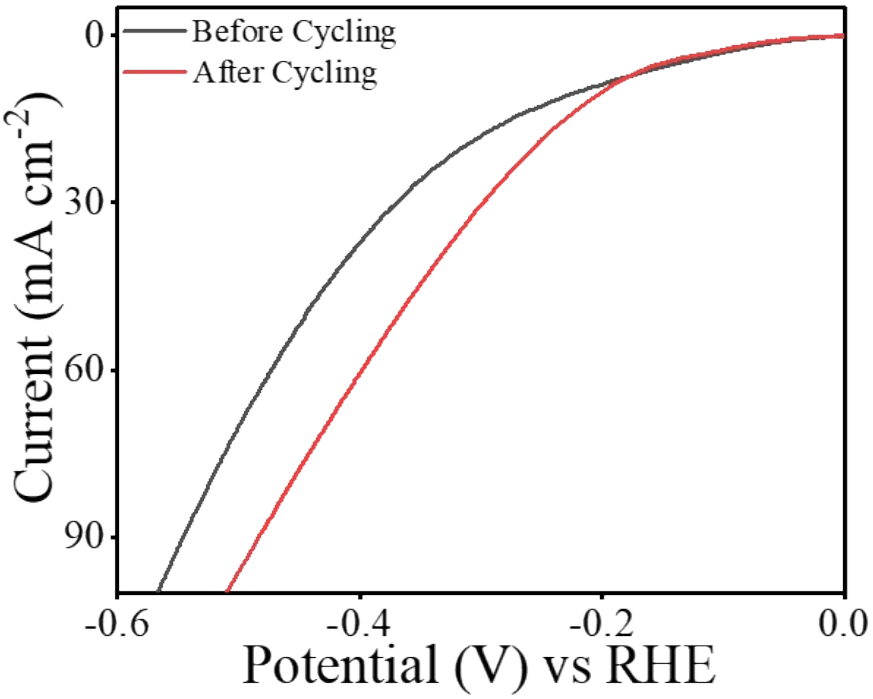

Figure S9. LSV profile of cp-HEAN before and after cycling.

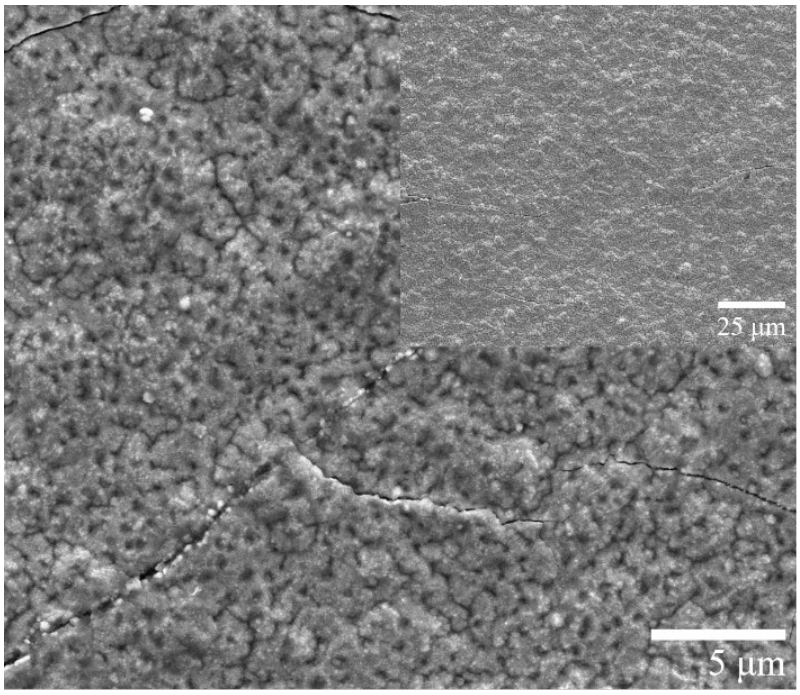

Figure S10. SEM images of cp-HEAN after cycling.

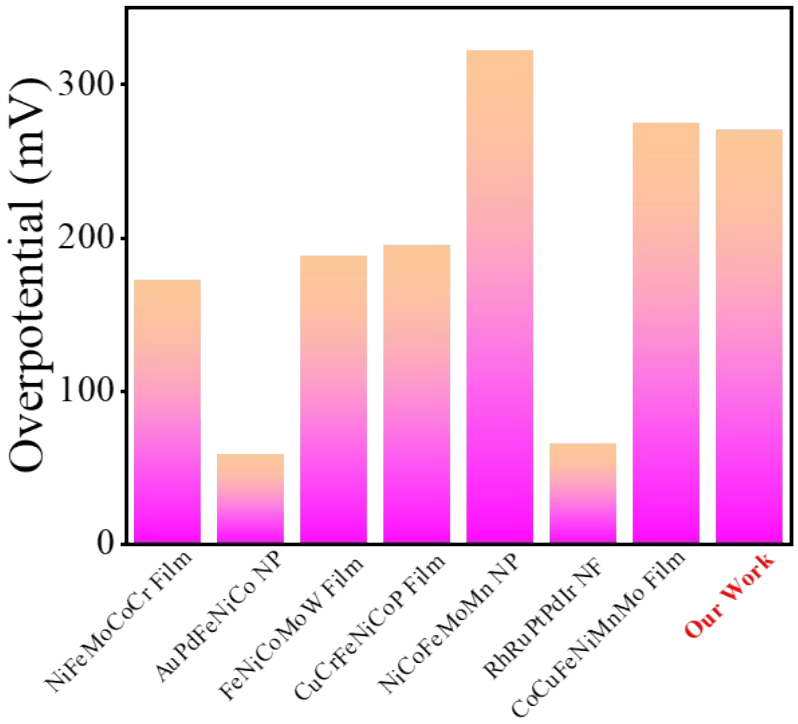

Figure S11. Overpotential comparison of our cp-HEAN with prior work.

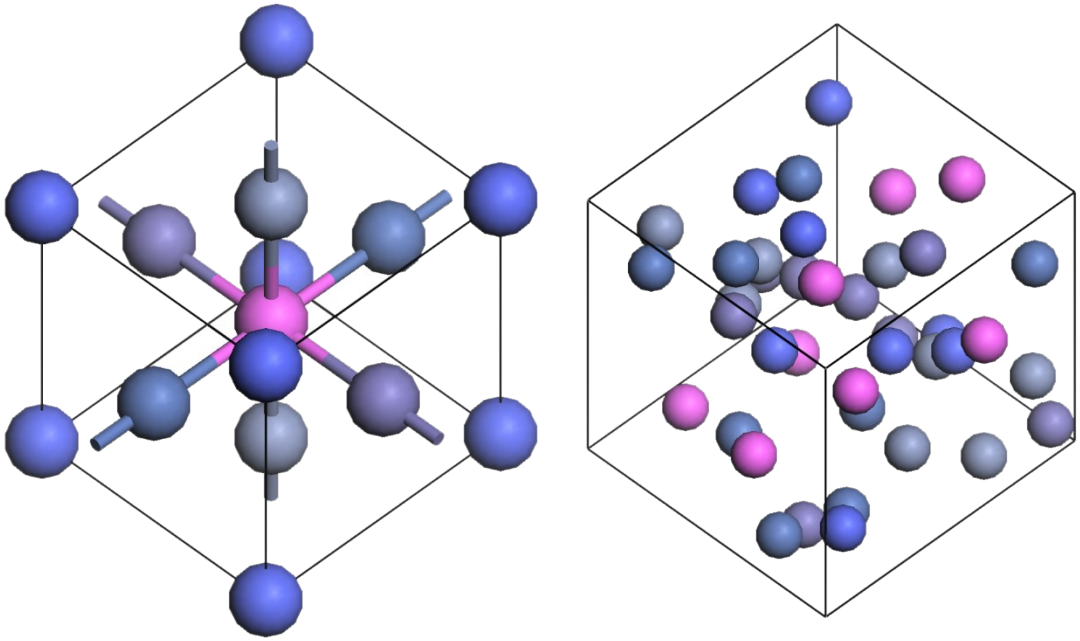

Figure S12. Optimized bulk structure models of crystalline HEA and amorphous HEA.

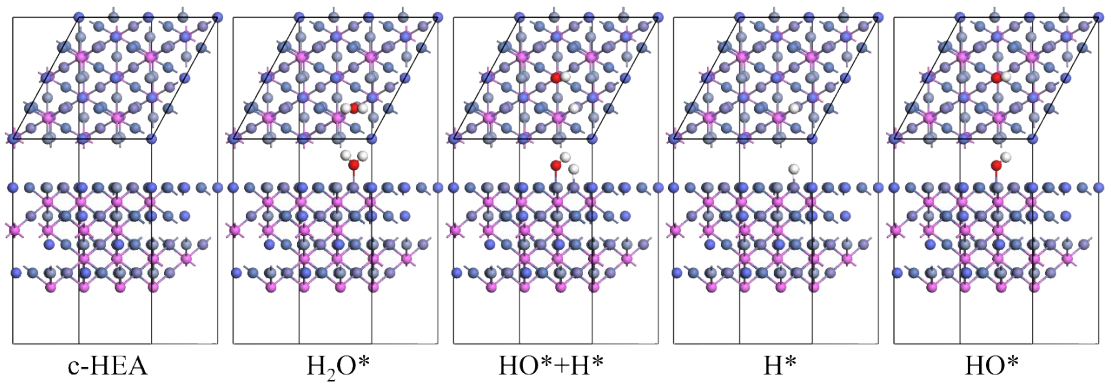

Figure S13. c-HEA with the adsorption of different species during HER process in alkaline media.

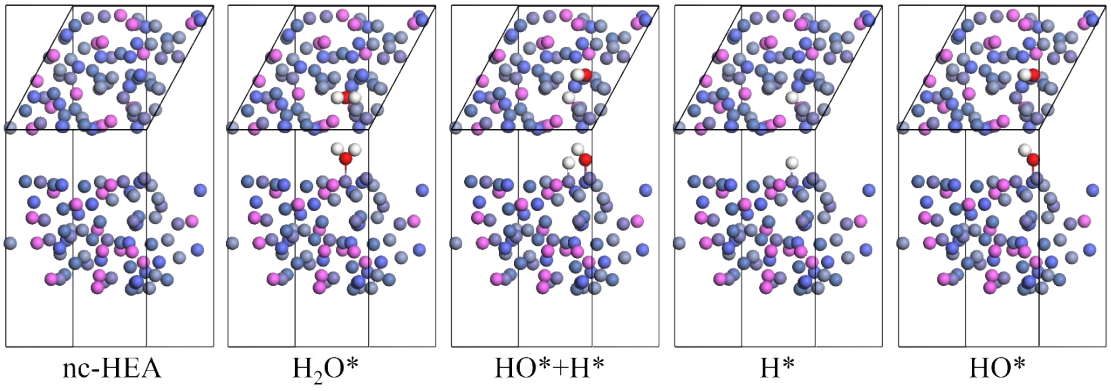

Figure S14. nc-HEA with the adsorption of different species during HER process in alkaline media.

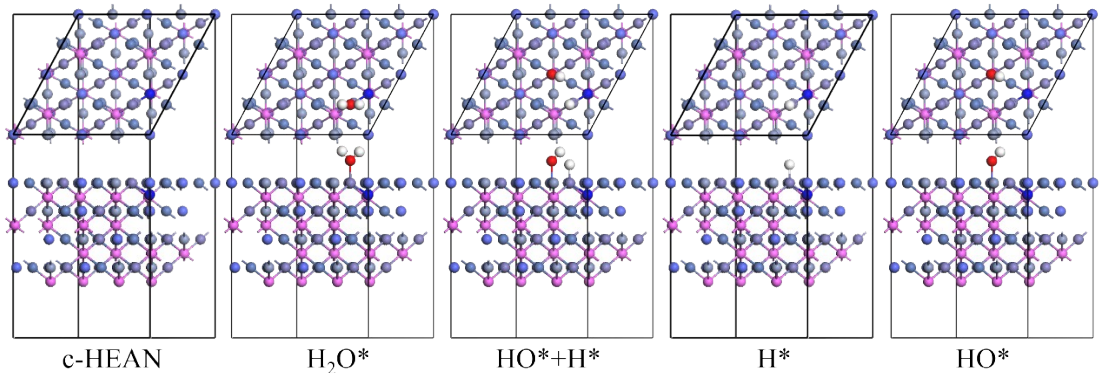

Figure S15. c-HEAN with the adsorption of different species during HER process in alkaline media.

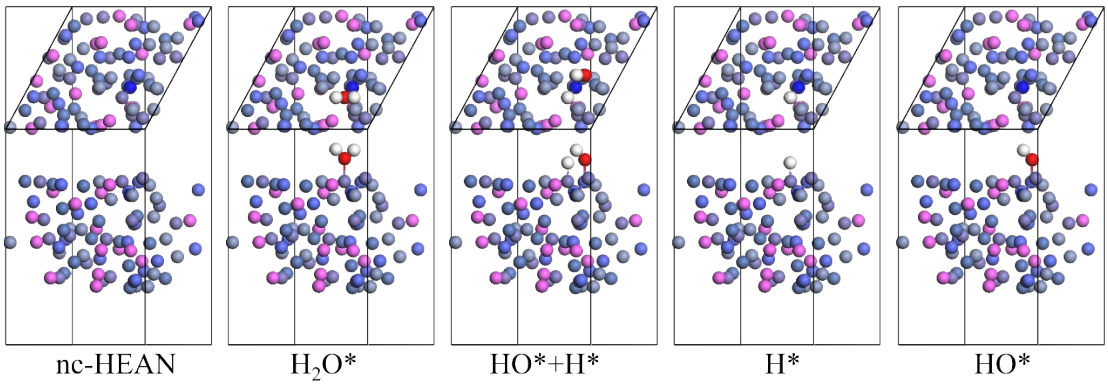

Figure S16. nc-HEAN with the adsorption of different species during HER process in alkaline media.

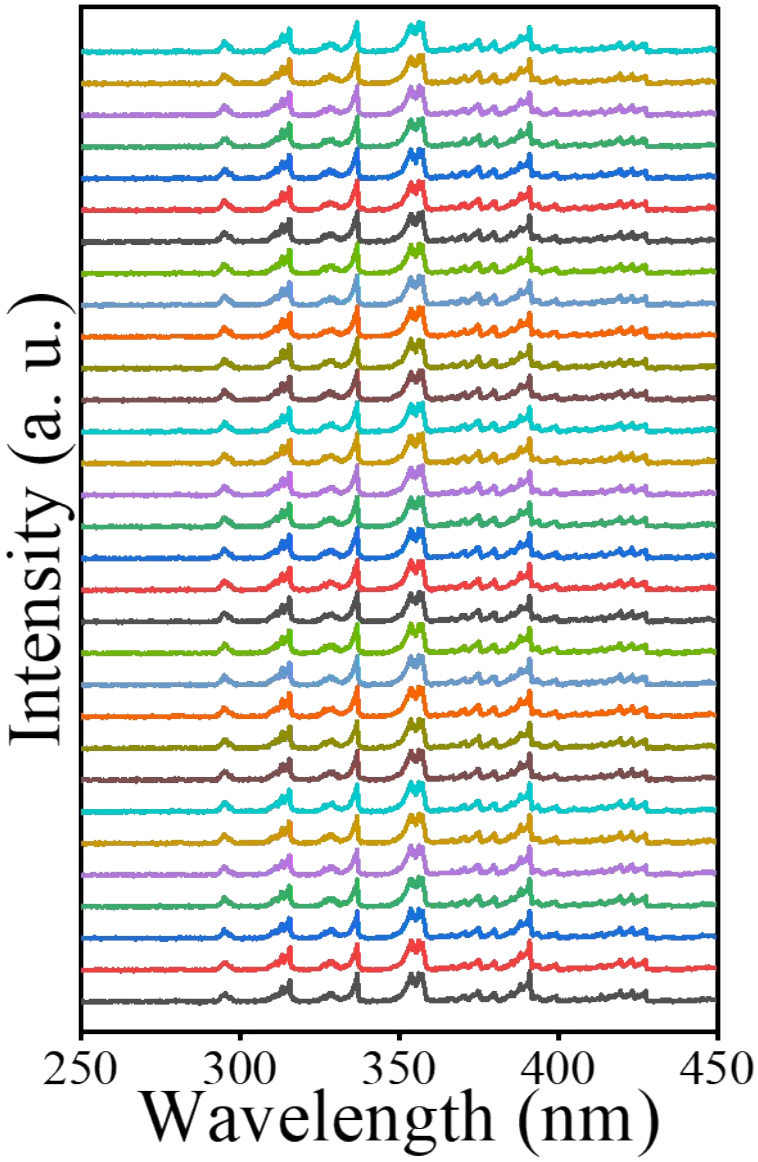

Figure S17. Time-resolved OES spectra during normal plasma processing for np-HEAN fabrication.

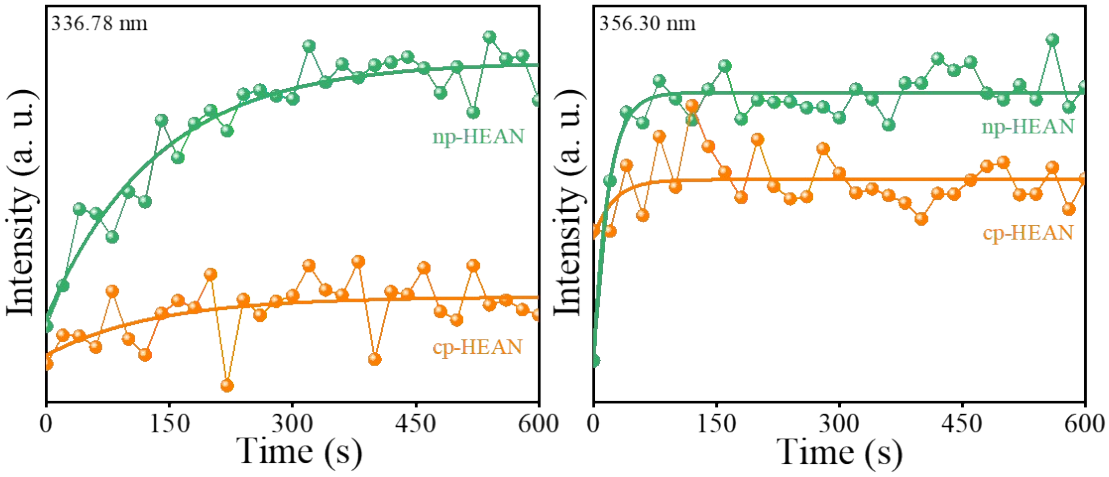

Figure S18. Peak intensity comparison of N-species at 336.78 and 356.30 nm